



Supplement of

A 20-year (1998–2017) global sea surface dimethyl sulfide gridded dataset with daily resolution

Shengqian Zhou et al.

Correspondence to: Ying Chen (yingchen@fudan.edu.cn)

The copyright of individual parts of the supplement might differ from the article licence.

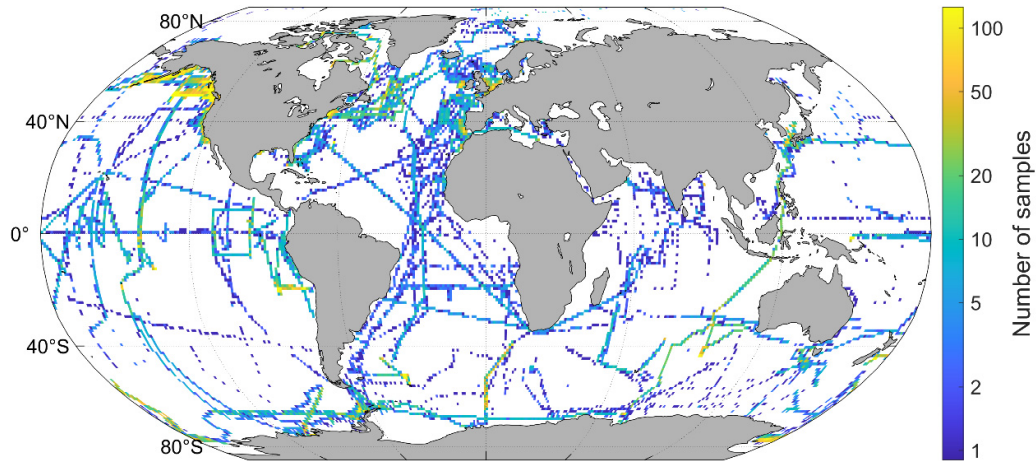


Figure S1. The spatial distribution of raw DMS observational data from the GSSD database and additional campaigns.

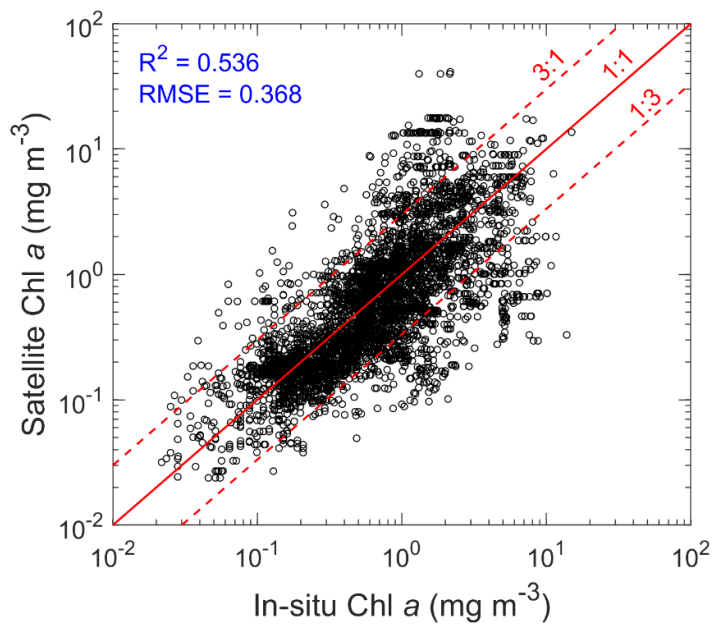


Figure S2. The comparison between the in-situ Chl *a* from GSSD database and the Copernicus-GlobColour Level-4 satellite-retrieved Chl *a* data. *n* is the number of samples. R^2 and RMSE correspond to \log_{10} space data.

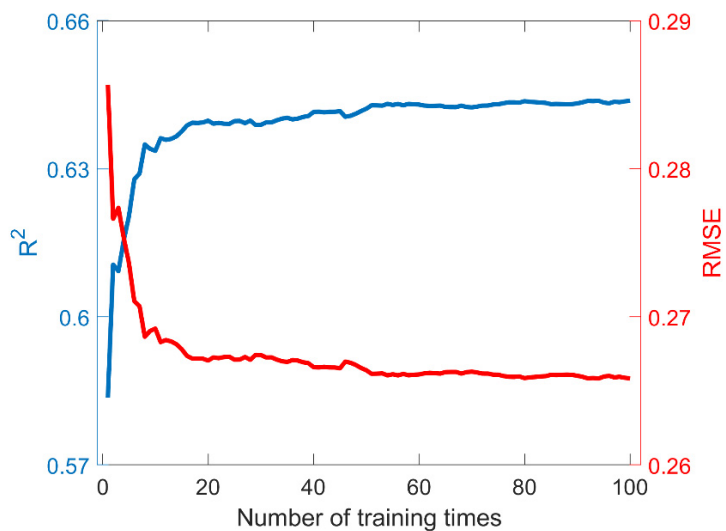


Figure S3. The changes of R^2 and RMSE between the averaged prediction results and observed DMS concentrations of the testing set along with the increase of training times.

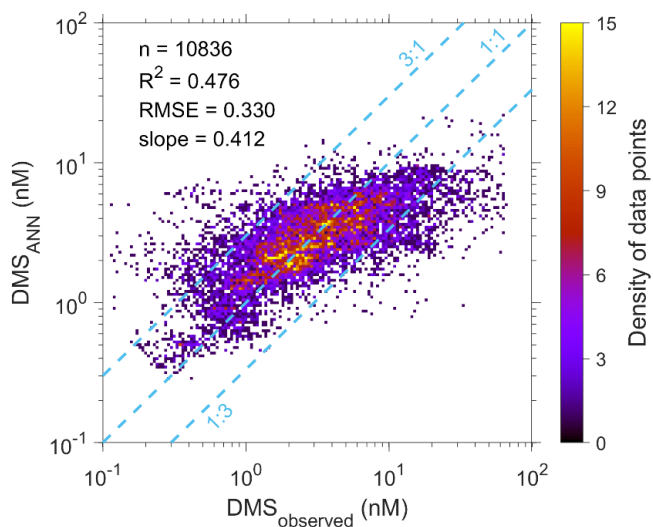


Figure S4. Scatter density plot for simulated versus observed DMS concentrations for all coastal samples employed in the ANN ensemble training.

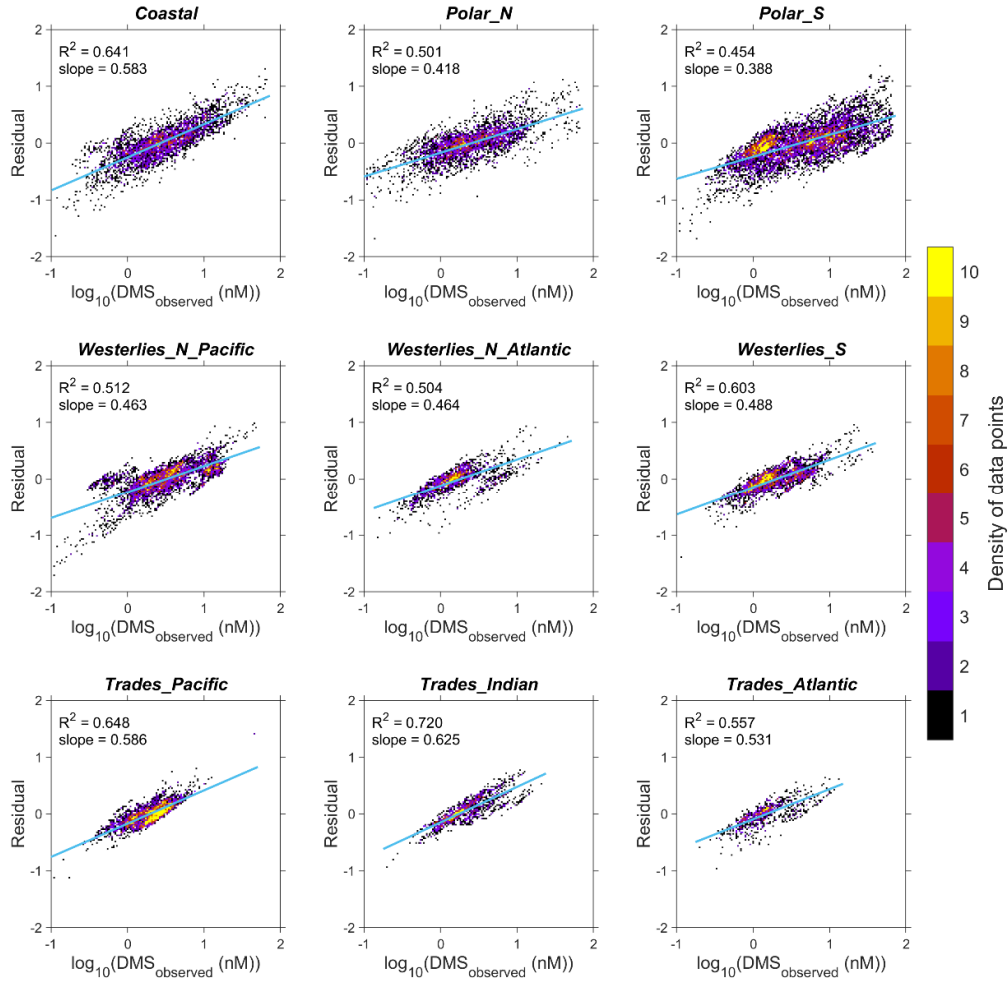


Figure S5. Scatter density plot for prediction residuals of $\log_{10}(\text{DMS})$ versus observed values in different regions corresponding to the samples used in ANN training.

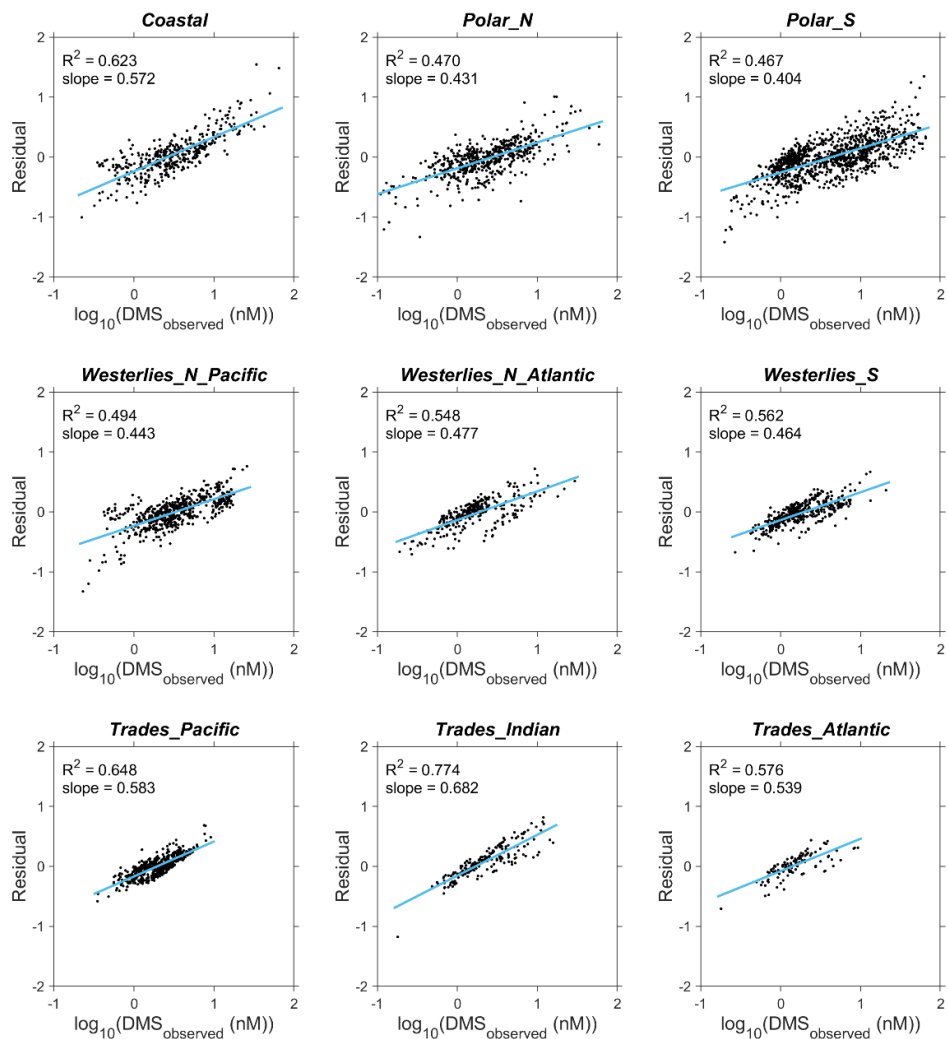


Figure S6. Correlations between prediction residuals of $\log_{10}(\text{DMS})$ and observed values across different regions corresponding to the testing set.

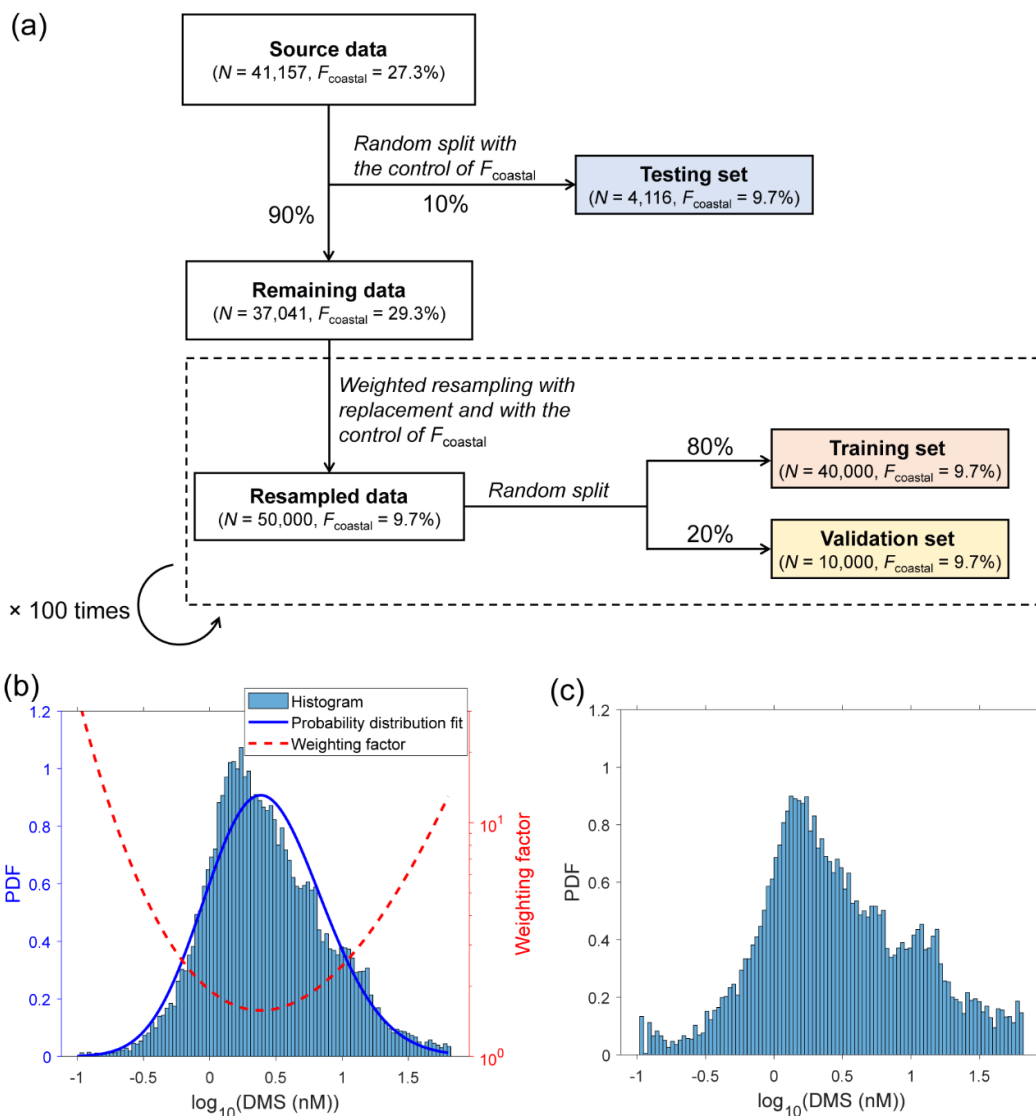


Figure S7. Data split and resampling strategy for ANN model training and testing. (a) Flowchart of the data split and resampling procedures. N and F_{coastal} denote the number of samples and the fraction of coastal samples, respectively. (b) The probability distribution of raw $\log_{10}(\text{DMS})$ values and the relationship between the weighting factor for weighted resampling and $\log_{10}(\text{DMS})$ value. PDF represents the probability density function. (c) The probability distribution of $\log_{10}(\text{DMS})$ values after weighted resampling.

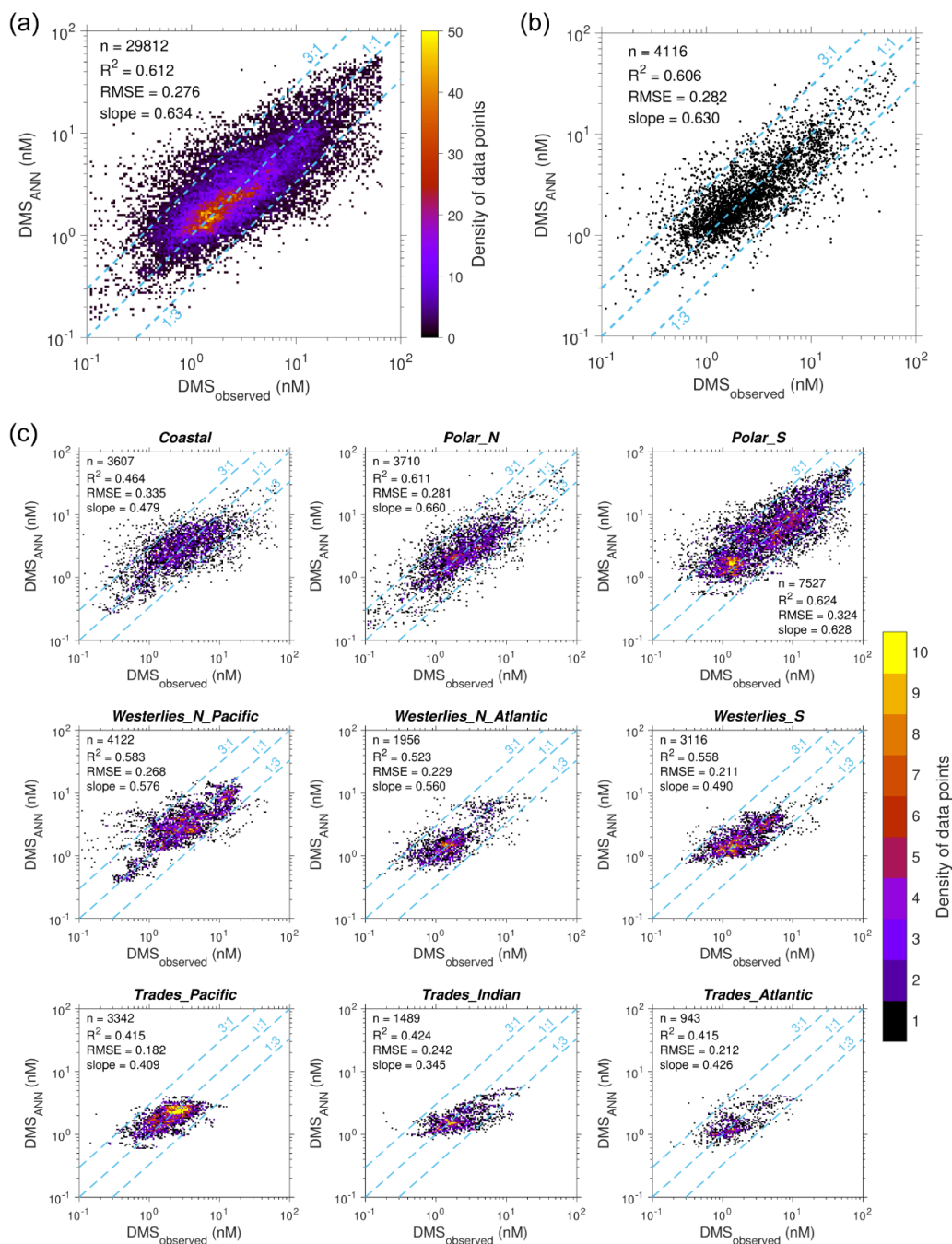


Figure S8. Comparisons between the simulated and observed DMS concentrations for the ANN model trained with the implementation of the weighted resampling strategy. (a) Scatter density for simulated versus observed DMS concentrations of the samples used in ANN training. (b) Comparison between the simulated versus observed DMS concentrations of testing set. (c) Comparison between the simulated versus observed DMS concentrations of the samples used in ANN training across 9 regions. The number of data points (n), \log_{10} space R^2 , root mean square error (RMSE), and linear regression slope are also displayed.

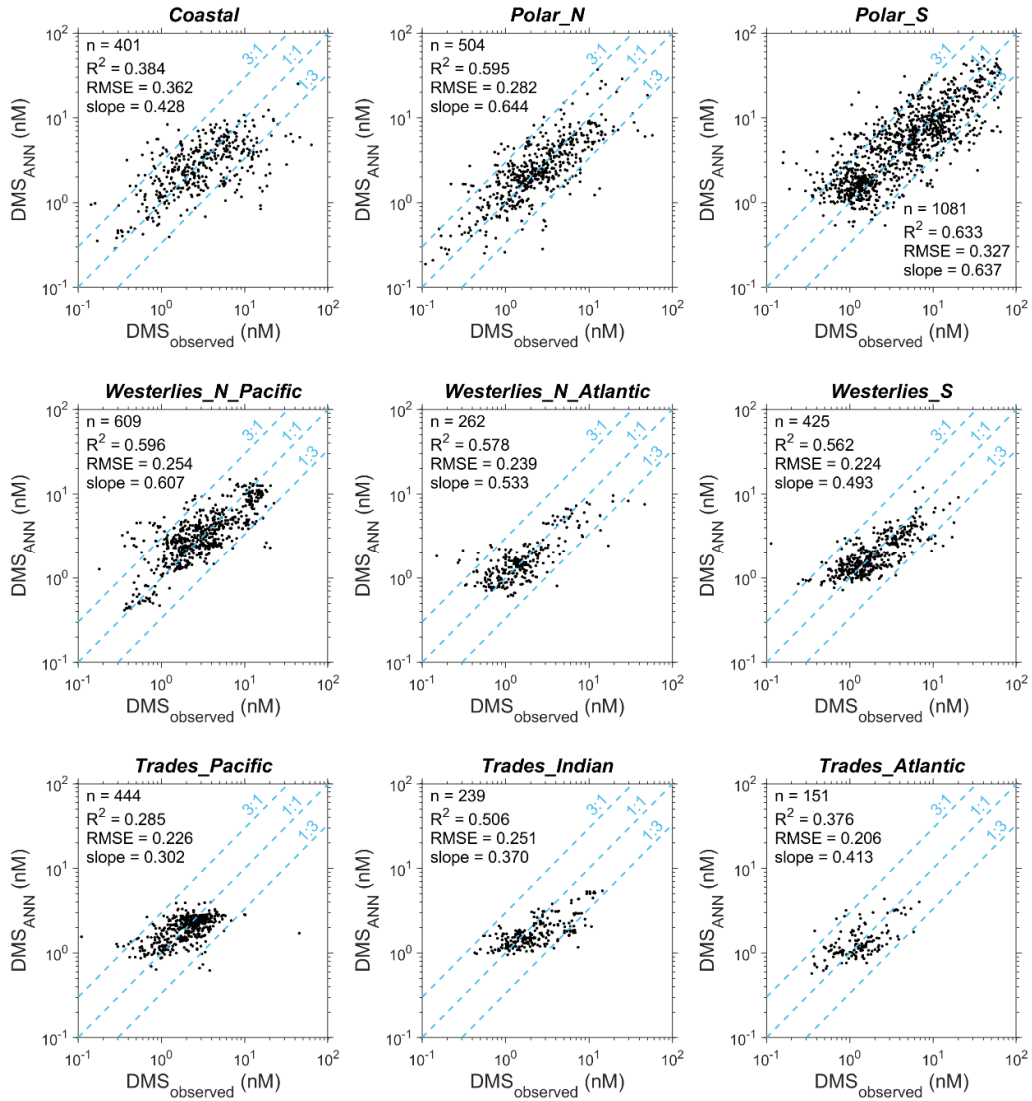


Figure S9. Comparison between the simulated versus observed DMS concentrations of the testing set across 9 regions. The ANN model is trained with the implementation of the weighted resampling strategy.

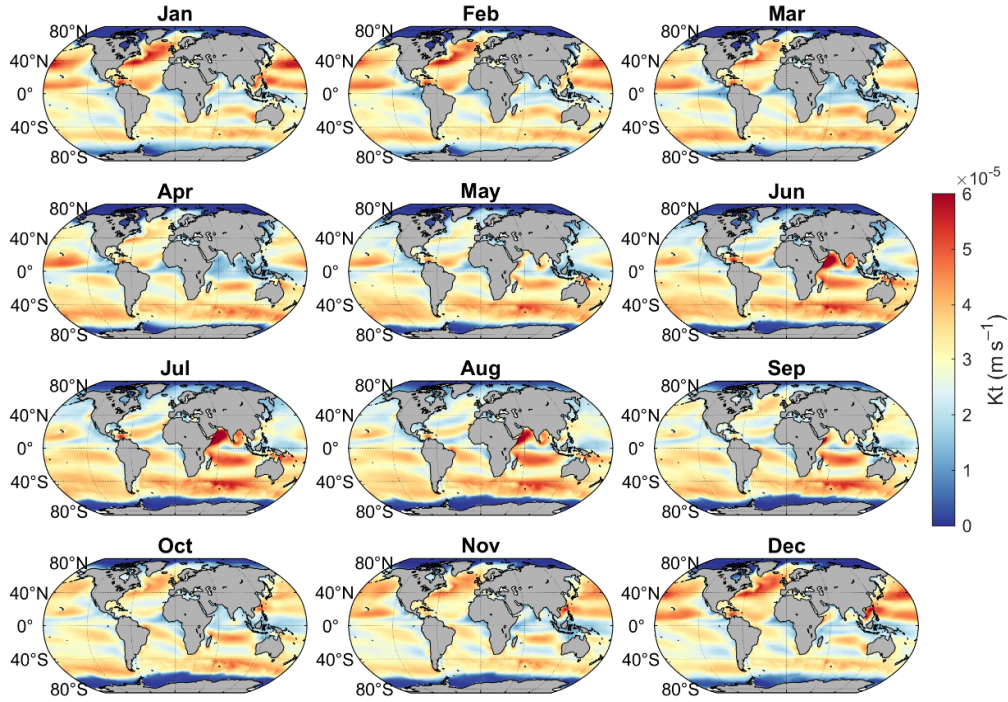


Figure S10. Monthly climatology of the total transfer velocity (Kt) of DMS from 1998 to 2017.

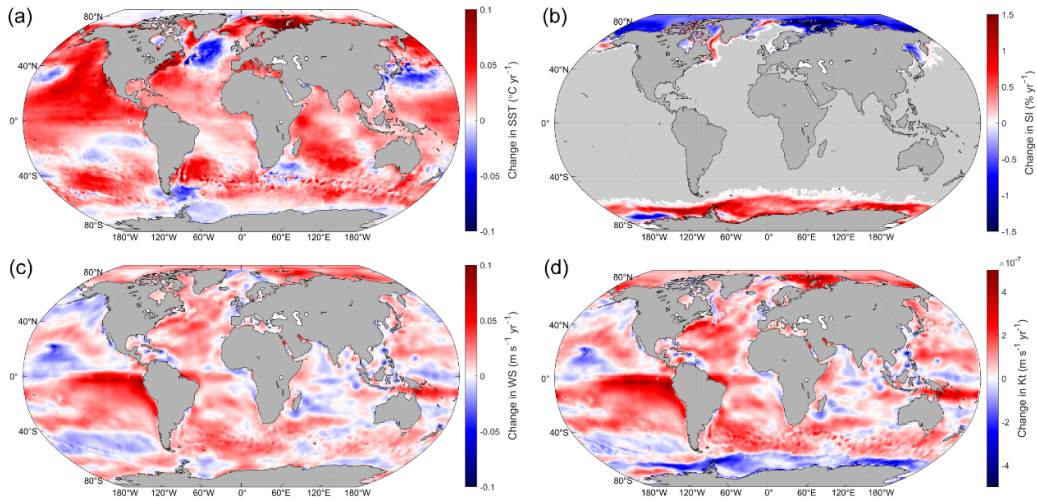


Figure S11. The spatial distributions of changes in (a) sea surface temperature (SST), (b) sea ice fraction (SI), and (c) surface wind speed (WS), and (d) DMS total transfer velocity (Kt) during 1998 to 2017.

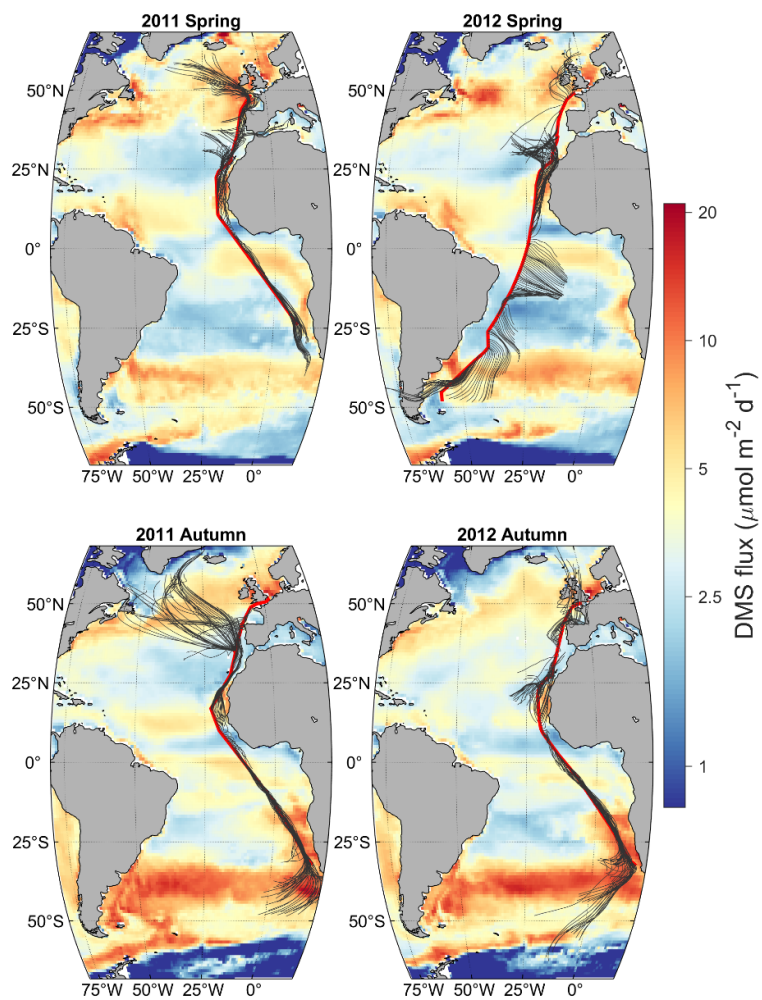


Figure S12. The ship tracks and 72-h air mass backward trajectories during four cruises in the Atlantic. The background is the average DMS flux during the time periods of each cruise based on Z23. The labelled seasons refer to seasons in the northern hemisphere.